Desalination and Water Treatment
www.deswater.com

doi: 10.5004/dwt.2018.21720

101 (2018) 61–69
January

Modification of (15,15) 2.034 nm diameter carbon nanotubes with long aliphatic chain and their desalination behavior

Qing Li[a,b,†], Dengfeng Yang[a,†], Jinsheng Shi[a], Jianhua Wang[a], Qingzhi Liu[a,*]

[a]*College of Chemistry and Pharmaceutical Science, Qingdao Agriculture University, No. 700 Changcheng Road, Qingdao City, 266109, China, Tel. +86-0532-86080895; emails: liuqz2001@163.com (Q. Liu), dfyang@qau.edu.cn (D. Yang), jsshiqn@163.com (J. Shi), 1140190376@qq.com (J. Wang)*
[b]*College of Chemistry, Beijing Normal University, Beijing 100875, China, email: liqing8282@163.com*

Received 22 June 2017; Accepted 19 November 2017

ABSTRACT

In order to imitate the structure of protein aquaporin-4 to improve salt rejection and to keep high water flux, long aliphatic chains were added at entrance or into interior of 2.034 nm (15,15) armchair carbon nanotubes (CNTs) and reverse osmosis membrane was built by simulation in this paper. The potential of mean force, conductance and axial density distributions of salt and water in CNTs was calculated. Results showed that under 200 MPa, salt rejection could be dramatically improved with high water flux (3.8–5.3 times higher than that of (8,8) unfunctionalized CNTs) when CNTs were modified with opposite groups or zwitterion groups at entrance. Certain numbers of short functional groups at entrance together with long aliphatic chain will improve both water permeation and salt rejection. For example, one pair of short chains ($CH_2NH_3^+$ and CH_2COO^-) and four 10-ammonioundecanote groups could make higher water flux than that with only four 10-ammonioundecanote groups and kept 100% salts rejection. CNTs with one pair of undecanoate and decan-1-aminium groups or two 6-ammonio-2-methylundecanedioate groups into interior can also obtain 100% salt rejection.

Keywords: Molecular dynamics simulation; Biomimetic modification; Reverse osmosis membrane; Carbon nanotube

1. Introduction

Freshwater scarcity has emerged as two-thirds of the world's population currently live in areas that experience water scarcity for at least 1 month a year [1]. Approximately more than 700 million people still lack access to safe drinking water after some measures to improve water resources [2]. Drawing clean freshwater from seawater has been a significant trend [3]. Reverse osmosis (RO) seawater desalination technology used for water treatment has been consistently developed to alleviate the water scarcity problem which is a rising seawater desalination technology in 21st century [4].

With excellent structural, mechanical and electronic properties, carbon nanotubes (CNTs) have attracted much attention since their discovery [5]. Recently, research found that CNTs could form into a nanoporous membrane structure used in water treatment [6–8]. Many experiments by various groups have also demonstrated unusually large water fluxes. Water permeate the CNTs freely with little resistance and the flow rates were found about 3–5 magnitude higher than theoretical calculation under hydrostatic pressure by previous simulations [9–11] and experiments [12,13]. Baek et al. [14] showed that the vertical alignment CNT membrane have a water flux approximately three times higher than the ultrafiltration membrane and water transport approximately 70,000 times faster than conventional non-slip flow [14]. By molecular simulation, Hummer et al. [9] discovered that water can permeate (6,6) CNT with slight resistance and the average water flux can be comparable with the flux of a biological counterpart, the aquaporin-1 channel. Also using

* Corresponding author.
† These two authors contributed equally in this article.

molecular simulation methods, Corry [15] and Thomas et al. [16] found that the number of water molecule entering into CNTs and the water flux increased with the enlargement of diameter. For example, only one water chain was observed in the (5,5) and (6,6) armchair CNTs, whereas a double chains were found in the (7,7) armchair CNTs and a quadruple chains emerged in the (8,8) armchair CNTs [15,17]. Our previous research found eight water chains in armchair (10,10) CNT [18] and more water chains in armchair (15,15) CNTs [19]. Meanwhile, the water flux of (15,15) 2.034 nm CNTs was 10 times the amount of flux of (8,8) [20] 1.085 nm CNTs, while salt rejection decreased sharply with the increase of CNTs' diameter. Functionalization can improve rejection properties of nanotubes according to the simulation [21–24] and experiment [6,25,26]. Corry [21] found that short functional groups ($–CH_2COO^-$, $–CH_2NH_3^+$ and $–CH_2CONH_2$) added at the entrance could improve desalination in (8,8) CNTs with the diameter about 1 nm. However, our previous simulating work [19] have proved that it was impossible for (15,15) CNTs with the diameter larger than 2 nm to achieve 100% salt rejection when they were modified with short chains ($–CH_2COO^-$ and $–CH_2NH_3^+$).

Due to the fact that the structure of CNTs' hydrophobic pores is similar to aquaporin-4 biological channels [27] what was the predominant biological water channel to expel all ions including proton and had six longer α spiral and two shorter α spiral [28], the longest one contained 23 amino acid residues and the shortest one contained 7 amino acid residues, CNTs modified with charged and polar long aliphatic chains to imitate the structure of protein aquaporin-4 were considered. Majumder and Corry's [29] simulating and experimental work showed that adding $Ru(bipy)_3^{2+}$ to CNTs could increase total electrostatic interaction of CNTs and affect water conduction. They also found that the addition of straight chain alkenes, anionic allyl charged dye molecules and aliphatic amine to the tip of CNTs could influence ions' transport. Chan's [30] simulating and experimental work showed that 1.5 nm diameter CNTs modified by long chain with zwitterions functional group at two ends could improve salt rejection.

In this paper, in order to improve the salt rejection and to keep high water flux, long-chain aliphatic groups were added to entrance or interior of CNTs to imitate the structure and characteristics of water channel protein.

2. Method

The CNTs membranes were modeled by hexagonally packed four CNTs following our previous methodology [31]. Each CNT was ~1.35 nm long as shown in Fig. 1. The CNTs axes were parallel to *z*-axis, and the CNTs' position was between z = 0 Å and z = 14 Å. The central position of CNTs is z = 7 Å. Periodic boundaries were used to form a continuous two-dimensional membrane. The CNTs were solvated by 2 nm TIP3P thick layer water on each side and Na^+ and Cl^- ions were randomly placed in the water layer to yield a net concentration of 250 mM and to neutralize the system.

Simulations were conducted using NAMD 2.9 [32] with the CHARMM27 [33] force field. The interaction between water ions and CNTs was calculated by Lennard–Jones equation:

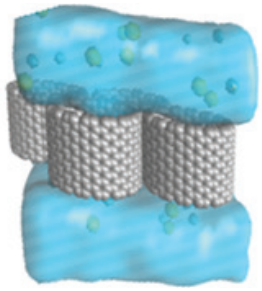

Fig. 1. The simulating system model formed by hexagonally packing four CNTs in a periodic cell and immersing in NaCl aqueous solution.

$$U_{\mathrm{LJ}} = \varepsilon_{ij}\left[\left(\frac{r_m}{r_{ij}}\right)^{12} - 2\left(\frac{r_m}{r_{ij}}\right)^{6}\right] + \frac{q_i q_j}{r_{ij}}$$

In this equation, ε_{ij} and r_m are parameters of Lennard–Jones and r_{ij} is the distance between two sites' distance, and q_i and q_j represent the particle i and j's charge. Langevin dynamics is employed to control the pressure and temperature. Time step is 1 fs. Cut off radius of non-bonded van der Waals interactions is 12 Å. The full electrostatic interactions were calculated by the particle mesh Ewald method. Before data collection, the system energy was minimized for 0.5 ns [20] under 1 atm constant pressure and at 300 K temperature.

All CNTs atoms except for functional groups were switched to be fixed to keep membrane in place. Two types of simulating techniques were adopted. First, 5 ns [34] hydrostatic pressure molecular dynamics simulations were conducted under 200 MPa to examine the water conduction and salt rejection mechanisms. Zhu et al.'s [35,36] method was employed to present a hydrostatic pressure difference during simulations. A constant force f was applied to produce a hydrostatic pressure difference across the two sides of the membrane along *z*-axis. The force was calculated by $\Delta P = nf/A$ formula, where n was the water molecular number in the force-applied section and A was the membrane cross-sectional area. Water and ions passing through the same modified CNT were calculated. The salts rejection were calculated by the ratio of the number of ion passing through the CNTs to the number of water molecules passing through the CNTs and was compared with the ratio of ions to water in the simulation system as a whole [16]. Second, potential of mean force (PMF) for Na^+ and Cl^- was determined using the method adaptive biasing forces [37] to generate quasi-equilibrium trajectory of particle motion. Uniform sampling [38] was used to determine PMF in the *z*-axial directions for ions and water in number, pressure, temperature ensemble. The PMF calculation covered the full length of the pore (position z = –0.5 to z = 2 nm) and the target positions were separated by 0.5 nm [31] in *z*-axial direction to improve the computing efficiency.

Different type of long aliphatic chains was shown in Fig. 2.

3. Results and discussion

3.1. Water transport in long-chain group functionalized CNTs

As seen in Table 1, the water flux of (15,15) 2.034 nm CNTs was 10 times high as that of (8,8) 1.085 nm CNTs [37]. However,

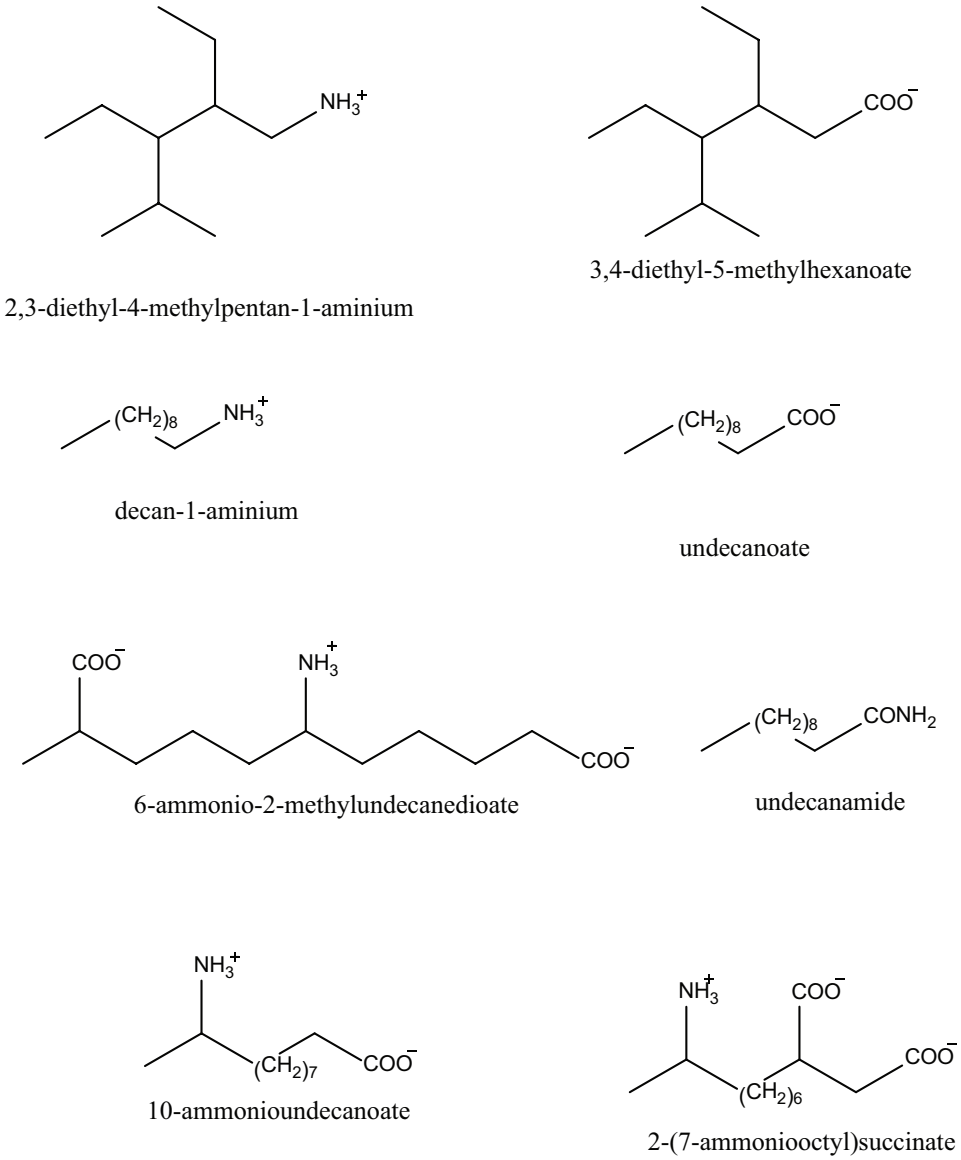

Fig. 2. Schematic of the molecules used for a functionalizing nanotube membrane.

Table 1
Numbers of ions and water molecules through the unfunctionalized or single charged long-chain group entrance-functionalized CNTs with in 5 ns under 200 MPa hydrostatic pressures

Tube type	Water flux	Water flux %	Na^+ permeation	Cl^- permeation	Na^+ rejection (%)	Cl^- rejection (%)
(8,8) Unfunctionalized	78.8 [28]	–	0.05	0.02	85.89	94.35
(15,15) Unfunctionalized	783.2	100	6	6.6	–	–
1-e $CH_3(CH_2)_9CO^{O}$–	403.6	51	0.8	0.4	55.95	77.98
1-e $CH_3(CH_2)_9NH_3^+$	814.2	103.96	5.2	4.8	–	–
1-e $CH_3(CH_2)_9CONH_2$	765.8	97.45	6.2	5.2	–	–
1-e $CH_3CH_2CH(CH(CH_3)_2)CH(CH_2CH_3)CH_2COO^-$	684	87.33	3	2	2.53	35.02
1-e $CH_3CH_2CH(CH(CH_3)_2)CH(CH_2CH_3)CH_2NH_3^+$	756.8	96.63	2.8	3.2	17.78	6.04

Note: Label 1-e represents the numbers of functionalized groups at entrance. The water flux % equal to the ratio of the water molecules number through functionalized CNTs to that through the unfunctionalized CNTs in one simulating system.

Na^+ and Cl^- could freely pass through the (15,15) CNTs. Our previous work [18] showed that it was difficult to achieve 100% salt rejection with short chains group (CH_2COO^- and $CH_2NH_3^+$) added into interior/at entrance of (15,15) CNTs. Considering that water channel protein had six longer α spiral and two shorter α spiral, the longest one contain 23 amino acid residues and the shortest one contain 7 amino acid residues, we added charged and polar groups with long aliphatic chain to entrance or interior of CNT to imitate water channel protein. The key results are summarized in Tables 1–4.

Although the water flux of functionalized CNTs was decreased (except for NH_3^+ group with long straight chain) compared with unfunctionalized case, the minimum water flux of functionalized CNTs was still 3.8 times higher than that of unfunctionalized (8,8) CNTs [20] and 37.8 [15] times of that of traditional RO membrane. The decrease of water flux was attributed to the steric blockages of the functional groups and by ions attracted by functional groups [21]. The number of water chains near the entrance of functionalized CNTs was smaller than that in unfunctionalized cases as shown in

Table 2
Numbers of ions and water molecules through the opposite charged long-chain entrance-functionalized CNTs with in 5 ns under 200 MPa hydrostatic pressure

Tube type	Water flux	Water flux%	Na^+ permeation	Cl^- permeation	Na^+ rejection (%)	Cl^- rejection (%)
1-e $CH_3(CH_2)_9COO^-$ 1-e $CH_3(CH_2)_9NH_3^+$	400.4	51.12	0.2	0.2	88.90	88.90
2-e $CH_3(CH_2)_9COO^-$ 2-e $CH_3(CH_2)_9NH_3^+$	429.8	54.88	0.4	0.4	79.32	79.32
1-e $CH_3CHNH_3^+(CH_2)_8COO^-$	448.2	57.23	0.8	0.2	60.34	90.08
2-e $CH_3CHNH_3^+(CH_2)_8COO^-$	460	12.92	1.4	0.8	12.17	12.17
4-e $CH_3CHNH_3^+(CH_2)_8COO^-$	407.4		0.4	0.2	78.18	89.09
1-e $CH_3CH(COO^-)(CH_2)_3$ $CH(NH_3^+)(CH_2)_4COO^-$	446.4	57.00	0.4	0.2	80.09	90.04
2-e $CH_3CH(COO^-)(CH_2)_3$ $CH(NH_3^+)(CH_2)_4COO^-$	490.6	62.64	0.4	0.2	81.88	90.94
4-e $CH_3CH(COO^-)(CH_2)_3$ $CH(NH_3^+)(CH_2)_4COO^-$	298.4	38.10	0	0.2	100	85.11

Table 3
Numbers of ions and water molecules through the long-chain and short-chain entrance-functionalized CNTs with in 5 ns under 200 MPa hydrostatic pressures

Tube type	Water flux	Water flux %	Na^+ permeation	Cl^- permeation	Na^+ rejection	Cl^- rejection
1-e $CH_3(CH_2)_9COO^-$ 1-e $CH_3(CH_2)_9NH_3^+$ +CH_2COO^- +$CH_2NH_3^+$	447	57.07	0.6	1	70.17	50.29
1-e $CH_3CHNH_3^+$ $(CH_2)_8COO^-$ +CH_2COO^- +$CH_2NH_3^+$	446.4	57.00	0.2	0.4	90.04	80.09
4-e $CH_3CHNH_3^+$ $(CH_2)_8COO^-$ +CH_2COO^- +$CH_2NH_3^+$	424.6	54.21	0	0	100	100
1-e $CH_3CH(COO^-)(CH_2)_3$ $CH(NH_3^+)(CH_2)_4COO^-$ +CH_2COO^- +$CH_2NH_3^+$	525.6	67.11	0.4	0.2	83.09	91.54
4-e $CH_3CH(COO^-)(CH_2)_3$ $CH(NH_3^+)(CH_2)_4COO^-$ +CH_2COO^- +$CH_2NH_3^+$	433.6	55.36	0.2	0	89.75	100

Table 4
Numbers of ions and water molecules through the interior-functionalized CNTs in 5 ns under 200 MPa hydrostatic pressures

Tube type	Water flux	Water flux %	Na^+ permeation	Cl^- permeation	Na^+ rejection (%)	Cl^- rejection (%)
2-m $CH_3CH(COO^-)(CH_2)_3CH(NH_3^+)(CH_2)_4COO^-$	334	42.65	0	0	100.00	100.00
1-m $CH_3(CH_2)_{90}COO^-$ 1-m $CH_3(CH_2)_9NH_3^+$	379.2	48.42	0	0	100	100

Note: Label 1-m represents the numbers of interior-functionalized groups.

Figs. 3(A)–(C). The ensemble-averaged axial density profiles analysis in Fig. 5 illustrated that water density was about 0.4 in functionalized CNTs, which was lower than 0.55 in unfunctionalized case. On the contrary, the positive charged groups (NH_3^+) with long straight aliphatic chain at entrance could increase water flux compared with unfunctionalized case. The reason was described as follows: the long-chain stayed outside of the CNTs during the whole simulating time and had no effect on hindering water molecule, thus the CNTs' effective diameter was equal to unfunctionalized CNTs as shown in Fig. 3(C). Moreover, the hydrophilic group NH_3^+ could alter the hydrophobic CNTs into a hydrophilic one and then attracted more water molecules at entrance and finally wet the hydrophilic CNTs [38] as shown in Figs. 3(C) and 5. The water density in the functionalized CNTs was 0.61, which was higher than 0.55 in unfunctionalized CNTs.

3.2. Ions transport in long-chain entrance-functionalized CNTs

3.2.1. Long chain with only one type of charged group

As shown in Table 1, positive charged group NH_3^+ or negative charged group COO^- or polar group $CONH_2$ with long linear aliphatic chain or branched aliphatic chain (both contain 10 carbon atoms) were added at entrance of the CNTs. The long linear aliphatic chain with negative COO^- group could achieve better rejection of Na^+ (56%) and Cl^- (78%) compared with that of polar group $CONH_2$ or positive charged group NH_3^+. COO^- repelled Cl^- but attracted Na^+ in tube as shown in Fig. 4(B) similar to CNTs modification with short chains COO^- group [18]. Na^+'s density peak was formed in corresponding position as shown in Fig. 5. The $CONH_2$ had no effect on salt rejection as shown in Table 1. While positive NH_3^+ with linear aliphatic chain had little influence on salt rejection because the chain stayed outside of the tube during the whole simulating time, Na^+ and Cl^- could pass through the CNTs freely as what happen in unfunctionalized case. When NH_3^+ or COO^- with branched aliphatic chain was added to the entrance, the rejection of Na^+ and Cl^- was improved but still not up to an ideal level.

3.2.2. Long chain with zwitterion/long chain with opposite groups (one chain with COO^- and another with NH_3^+)

Since long linear aliphatic NH_3^+ groups can improve water flux and long linear aliphatic COO^- groups can improve salt rejection, we wonder if the long opposite groups (one with COO^- and another with NH_3^+) or certain long zwitterion (group with both COO^- and NH_3^+) added to the entrance could improve both salt rejection and water

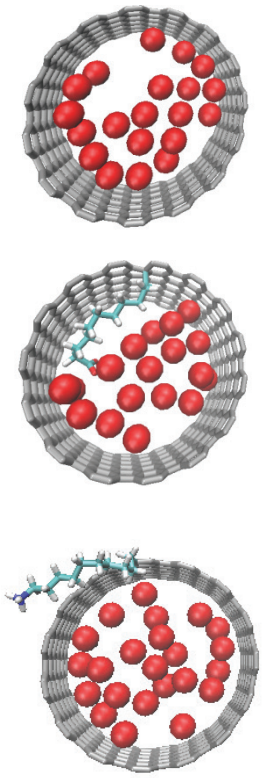

Fig. 3. Water chains in CNT with 2.034 nm diameter (15,15), the red ball represent O^{2-} (A) unfunctionalized CNTs, (B) CNTs modification with negative charged groups (COO^-) combination with long straight aliphatic chain and (C) CNTs modification combination with positive charged groups (NH_3^+) with long straight aliphatic chain.

flux. The results are shown in Table 2. When zwitterion group 6-ammonio-2-methylundecanedioate or 10-ammonioundecanote, compared with the CNTs modified with only undecanoate groups, were added to the entrance of CNTs, both water flux and salt rejection were about 11% higher undecanoate group and decan-1-aminium group added to the entrance could also improve salt rejection 89% with high water flux (water kept no change).

When four 6-ammonio-2-methylundecanedioate groups were added to the entrance, 100% Na^+ rejection and 85% Cl^- rejection were achieved. The four 6-ammonio-2-methylundecanedioate groups did prevent Na^+ ion from passing through, which because Na^+ was trapped by the strong attraction of COO^- groups at entrance, as shown in Fig. 4(D). In this case, Cl^- could partly pass through, which because the interaction

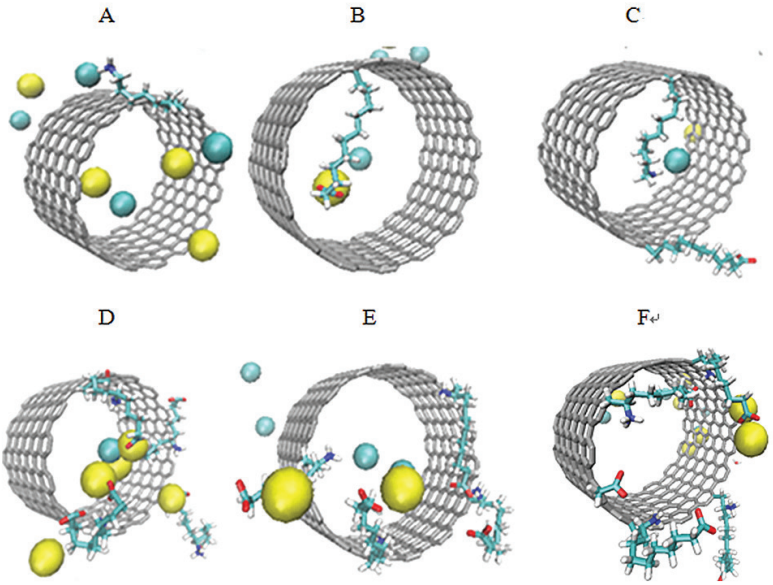

Fig. 4. Chart of Na^+ (yellow) and Cl^- (blue) ions near the functional group of the functionalized CNTs. Results are shown for the CNTs with (A) long-chain NH_3^+, (B) long-chain COO^-, (C) long-chain NH_3^+ and COO^-, (D) four 6-ammonio-2-methylundecanedioate groups, (E) four 10-ammonioundecanote groups and (F) four 10-ammonioundecanote groups together with a couple of short chains (NH_3^+ and COO^-).

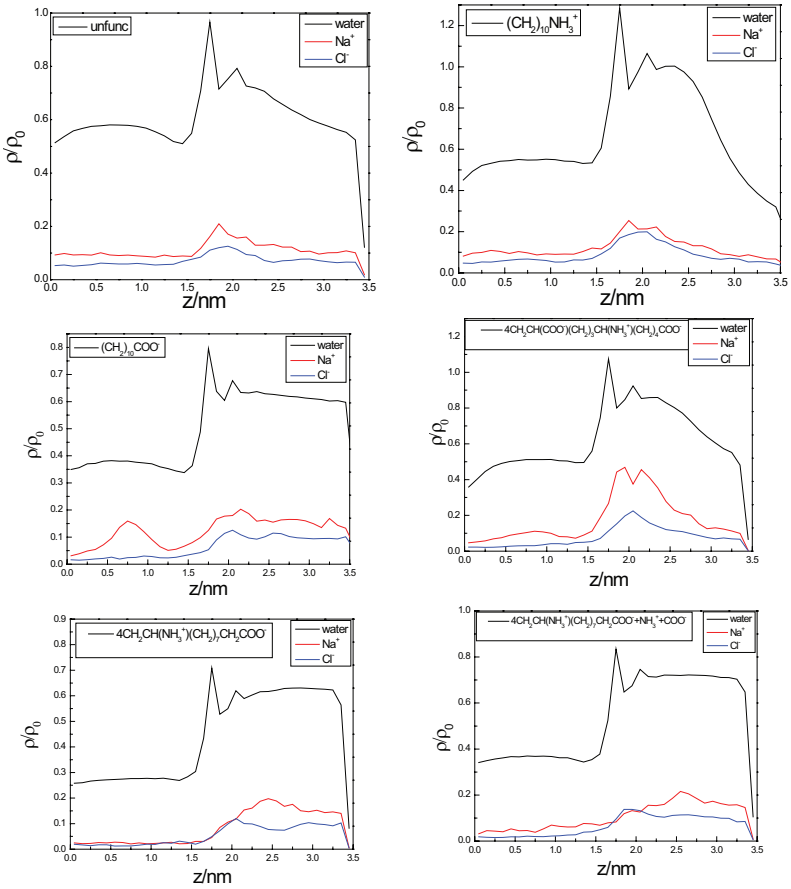

Fig. 5. *z*-Axis density map of Na^+ (blue line), Cl^- (red line) and water's (black line) of carbon nanotubes under 200 MPa hydrostatic pressure (*z* represents the axis of CNT). The position from $z = 0$ to $z = 1.4$ nm is the location of CNTs.

between NH_3^+ and Cl^- was lower than that between COO^- and Na^+ as shown in Fig. 7. The PMF in Fig. 6(A) illustrates that Na^+ was trapped at the modified position by strong attraction of $–COO^-$ with 2.08 kcal/mol force, which finally led to 100% desalination of Na^+. While Cl^- met 0.76 kcal/mol force near the entrance.

3.2.3. Long-chain and short-chain entrance-functionalized CNTs

Some simulations [18,34] indicated that CNTs modified with short charged or polar groups (CH_2COO^-, $CH_2NH_3^+$ and $CONH_2$) with short chains at entrance of small diameter CNTs (about 1 nm) could block ions. Could the charged long straight aliphatic chain together with charged short chain improve salt rejection on the basic of higher water flux? As the results shown in Table 3, proper addition of charged short chain with charged long chain did improve salts rejection. For example, the CNTs modified with four 10-ammonioundecanote groups and a pair of short chains charged groups (CH_2COO^- and $CH_2NH_3^+$) could obtain 100% salts rejection with 4.2% water flux improvement. As seen in Fig. 8, Na^+ met 1.17 kcal/mol force near the entrance and was trapped by strong attraction of $–COO^-$ at 1.17 kcal/mol force, which finally led to 100% rejection of Na^+. Cl^- met 0.45 force near the entrance higher than that with only four 10-ammoniounde-canote groups. In this case, Cl^- had no chance to enter into the CNT and result in 100% rejection. One 6-ammonio-2-methylundecanedioate group and a couple of short charged groups

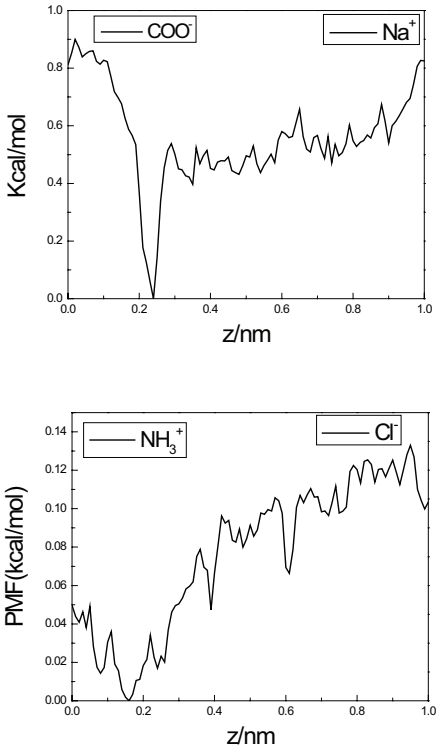

Fig. 7. PMF (potential of mean force) of Na^+ ion and COO^- group, Cl^- ion and NH_3^+ group. The position of COO^- or NH_3^+ groups is z = 0 nm.

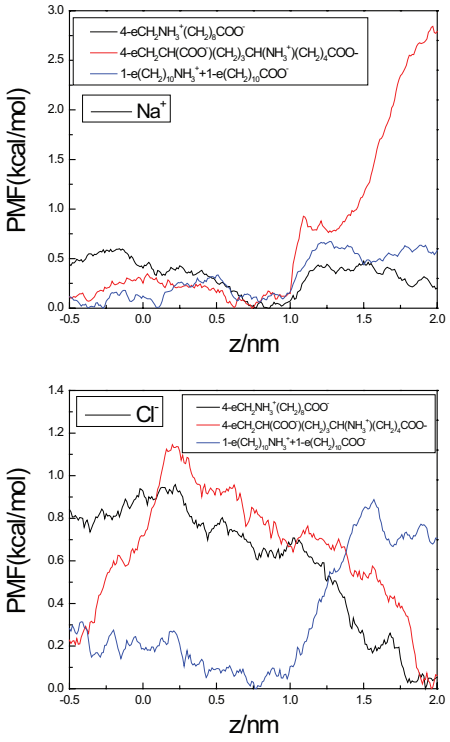

Fig. 6. PMF (potential of mean force) for Na^+, Cl^- in (15,15) modified CNTs, the ion was moved from the bulk solution (z = 2.0) to the next bulk solution (z = –0.5) in each case, the CNTs are located from z = 0 to z = 1.4 nm.

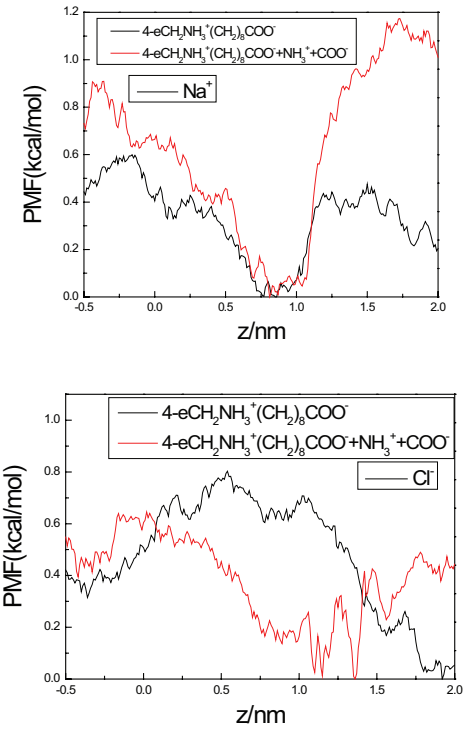

Fig. 8. PMF (potential of mean force) for Na^+, Cl^- in (15,15) modified CNTs, the ion was moved from the bulk solution (z = 2.0) to the next bulk solution (z = –0.5) in each case, the CNTs are located from z = 0 to z = 1.4 nm.

(CH_2COO^- and $CH_2NH_3^+$) also improved both water flux and salt rejection.

3.3. Ions transport in opposite charged and zwitterion long-chain interior-functionalized CNTs

Our previous work [18,19] indicated that salt rejection of CNTs modified with short groups (CH_2COO^- and $CH_2NH_3^+$) in interior was higher than that at entrance with slight decrease of water conduction. Two 6-ammonio-2-methylundecanedioate groups or a pair of undecanoate and decan-1-aminium groups were added to interior of CNTs to investigate water flux and salts rejection. The results showed that interior modified CNTs with long straight charged groups could achieve 100% salts rejection as shown in Table 4. When a pair of undecanoate and decan-1-aminium groups was added at entrance of the CNTs, the two chains were alternatively extended into the CNTs during most simulating time seen in Fig. 4(C). While the interior two chains were always stay inner of CNTs and result in smaller space of CNT pore. Na^+ and Cl^- had no chance to enter the CNT due to the repellency of charged groups and the limited space in this case, as shown in Fig. 9. PMF curves showed that Na^+ faced 0.66 kcal/mol and Cl^- faced 0.68 kcal/mol force at the middle of CNTs in Fig. 10. The ensemble-averaged axial density profiles analysis in Fig. 11(A) illustrated that ion density was close to 0 because no ions permeated the CNTs. When two 6-ammonio-2-methylundecanedioate groups were added to interior of CNTs, the ensemble-averaged axial density profiles analysis in Fig. 11 illustrated that Na^+ formed a density peak at entrance while Cl^- did not. Because the COO^- groups could attract two Na^+ ions to the mouth of the pore and repel the same charged Cl^- ions seen in Fig. 9. The blockage of Na^+ ions and long-chain group together with the repulsion of NH_3^+ prevented more Na^+ ion from entering to the CNTs. Then, the CNTs achieved 100% salts rejection.

4. Conclusion

To imitate the predominant biological water channel – aquaporins, different charged and polar functional groups with long aliphatic chain were added to entrance or interior

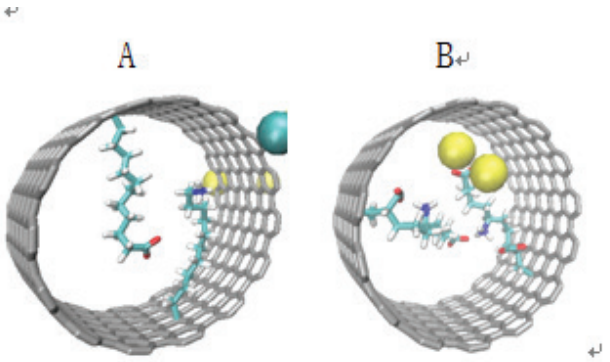

Fig. 9. Chart of Na^+ (yellow) and Cl^- (blue) ions near the functional group of the functionalized CNTs. Results are shown for CNTs with (A) a couple of undecanoate and decan-1-aminium groups and (B) two 6-ammonio-2-methylundecanedioate groups.

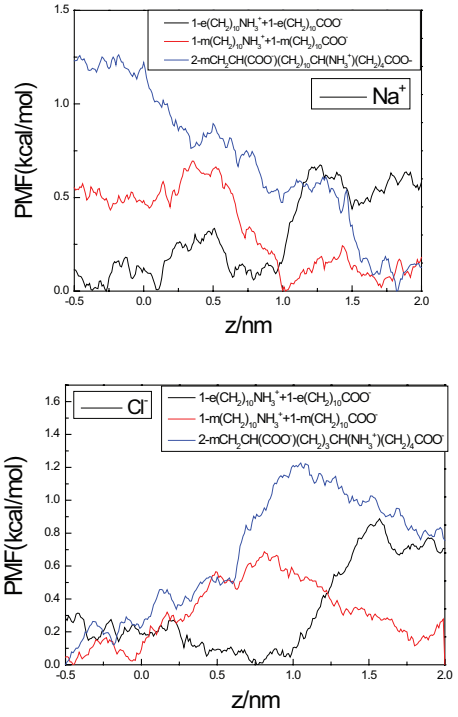

Fig. 10. PMF (potential of mean force) for Na^+, Cl^- in (15,15) modified CNTs, the ion was moved from the bulk solution (z = 2.0) to the next solution (z = –0.5) in each case, the CNTs are located from z = 0 to z = 1.4 nm.

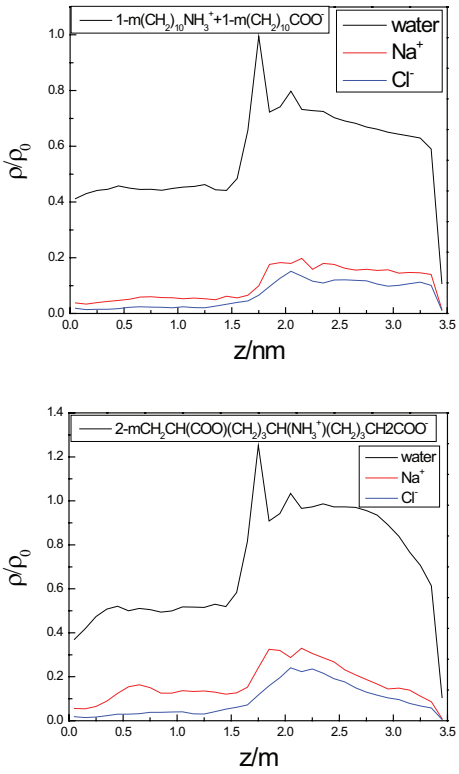

Fig. 11. z-Axis density map of Na^+ (blue line), Cl^- (red line) and water's (black line) of carbon nanotubes under 200 MPa hydrostatic pressure.

of the (15,15) CNTs with diameter larger than 2 nm system to obtain high salt rejection and water flux. The results showed that the lowest water flux of 100% rejection modified (15,15) CNTs was about 37.8 times of that of traditional RO membrane and 4.2 times of unmodified 1.1 nm diameter (8,8) CNTs. 100% salts rejection could be achieved with a couple of undecanoate and decan-1-aminium groups or two 6-ammonio-2-methylundecanedioate groups added into interior of CNTs or four 10-ammonioundecanote groups combination with a couple of short chains ($CH_2NH_3^+$ and CH_2COO^-) in the entrance without affecting water permeation evidently.

Acknowledgment

This work was supported by the National Natural Science Foundation of China (No. 21306096).

References

[1] U.N.E. Programme, World Water Area (WWA) Programme, The United Nations World Water Development Report 2017, Wastewater: The Untapped Resource, 2017.
[2] World Health Organization. II.UNICEF (WUJE), Supply, Progress on Drinking-Water and Sanitation – 2014 Update, 2014.
[3] Q. Chen, L. Meng, Q. Li, D. Wang, W. Guo, Z. Shuai, L. Jiang, Water transport and purification in nanochannels controlled by asymmetric wettability, Small, 7 (2011) 2225–2231.
[4] Y. Zhou, S. Yu, C. Gao, Reverse osmosis composite membrane (I) chemical structure and performance, J. Chem. Ind. Eng., 6 (2006) 18.
[5] S. Iijima, Helical microtubules of graphitic carbon, Nature, 354 (1991) 56–58.
[6] B.J. Hinds, N. Chopra, T. Rantell, R. Andrews, V. Gavalas, L.G. Bachas, Aligned multiwalled carbon nanotube membranes, Science, 303 (2004) 62.
[7] D. Zhang, L. Shi, J. Fang, K. Dai, J. Liu, Influence of carbonization of hot-pressed carbon nanotube electrodes on removal of NaCl from saltwater solution, Mater. Chem. Phys., 96 (2006) 140–144.
[8] D. Zhang, L. Shi, J. Fang, K. Dai, Influence of diameter of carbon nanotubes mounted in flow-through capacitors on removal of NaCl from salt water, J. Mater. Sci., 42 (2007) 2471–2475.
[9] G. Hummer, J.C. Rasaiah, J.P. Noworyta, Water conduction through the hydrophobic channel of a carbon nanotube, Nature, 414 (2001) 188.
[10] A. Striolo, The mechanism of water diffusion in narrow carbon nanotubes, Nano Lett., 6 (2006) 633.
[11] A. Kalra, S. Garde, G. Hummer, From the cover: osmotic water transport through carbon nanotube membranes, Proc. Natl. Acad. Sci. USA, 100 (2003) 10175.
[12] J.K. Holt, H.G. Park, Y. Wang, M. Stadermann, A.B. Artyukhin, C.P. Grigoropoulos, A. Noy, O. Bakajin, Fast mass transport through sub-2-nanometer carbon nanotubes, Science, 312 (2006) 1034–1037.
[13] M. Majumder, N. Chopra, R. Andrews, B.J. Hinds, Nanoscale hydrodynamics: enhanced flow in carbon nanotubes, Nature, 438 (2005) 44.
[14] Y. Baek, C. Kim, K.S. Dong, T. Kim, J.S. Lee, H.K. Yong, K.H. Ahn, S.B. Sang, C.L. Sang, J. Lim, High performance and antifouling vertically aligned carbon nanotube membrane for water purification, J. Membr. Sci., 460 (2014) 171–177.
[15] B. Corry, Designing carbon nanotube membranes for efficient water desalination, J. Phys. Chem. B, 112 (2008) 1427–1434.
[16] M. Thomas, B. Corry, T.A. Hilder, What have we learnt about the mechanisms of rapid water transport, ion rejection and selectivity in nanopores from molecular simulation? Small, 10 (2014) 1453–1465.
[17] A. Striolo, P.K. Naicker, A.A. Chialvo, P.T. Cummings, K.E. Gubbins, Simulated water adsorption isotherms in hydrophilic and hydrophobic cylindrical nanopores, Adsorption, 11 (2005) 397–401.
[18] Q. Li, D. Yang, J. Shi, X. Xu, S. Yan, Q. Liu, Biomimetic modification of large diameter carbon nanotubes and the desalination behavior of its reverse osmosis membrane, Desalination, 379 (2016) 164–171.
[19] Q. Li, D.F. Yang, J.H. Wang, Q. Wu, Q.Z. Liu, Biomimetic modification and desalination behavior of (15,15) carbon nanotubes with a diameter larger than 2 nm, Acta Phys. Chim. Sin., 32 (2016) 691–700.
[20] C. Song, B. Corry, Intrinsic ion selectivity of narrow hydrophobic pores, J. Phys. Chem. B, 113 (2009) 7642–7649.
[21] B. Corry, Water and ion transport through functionalised carbon nanotubes: implications for desalination technology, Energy Environ. Sci., 4 (2011) 751–759.
[22] F. Fornasiero, H.G. Park, J.K. Holt, M. Stadermann, C.P. Grigoropoulos, A. Noy, O. Bakajin, Ion exclusion by sub-2-nm carbon nanotube pores., Proc. Natl. Acad. Sci. USA, 105 (2008) 17250–17255.
[23] F. Fornasiero, J.B. In, S. Kim, H.G. Park, Y. Wang, C.P. Grigoropoulos, A. Noy, O. Bakajin, pH-tunable ion selectivity in carbon nanotube pores, Langmuir, ACS J. Surf. Colloids, 26 (2010) 14848–14853.
[24] Z.E. Hughes, C.J. Shearer, J. Shapter, J.D. Gale, Simulation of water transport through functionalized single-walled carbon nanotubes (SWCNTs), J. Phys. Chem. C, 116 (2012) 24943–24953.
[25] M. Majumder, N. Chopra, B.J. Hinds, Mass transport through carbon nanotube membranes in three different regimes: ionic diffusion and gas and liquid flow, ACS Nano, 5 (2011) 3867–3877.
[26] M. Majumder, X. Zhan, R. Andrews, B.J. Hinds, Voltage gated carbon nanotube membranes, Langmuir, ACS J. Surf. Colloids, 23 (2007) 8624–8631.
[27] Y. Cui, D.A. Bastien, Water transport in human aquaporin-4: molecular dynamics (MD) simulations, Biochem. Biophys. Res. Commun., 412 (2011) 654–659.
[28] S. Haixin, R. Gang, H. Tingjun, X. Xiaojie, T. Guoca, S. Jiushu, C. Lihe, P. Xiaofeng, W. Shikang, H. Guangye, Structure and mechanism of water channels, Progr. Chem., Beijing, 16 (2004) 145–152.
[29] M. Majumder, B. Corry, Anomalous decline of water transport in covalently modified carbon nanotube membranes, Chem. Commun., 47 (2011) 7683–7685.
[30] W. Chan, H. Chen, A. Surapathi, M.G. Taylor, X. Shao, E. Marand, J.K. Johnson, Zwitterion functionalized carbon nanotube/polyamide nanocomposite membranes for water desalination, ACS Nano, 7 (2013) 5308–5319.
[31] D. Yang, Q. Liu, H. Li, C. Gao, Molecular simulation of carbon nanotube membrane for Li^+ and Mg^{2+} separation, J. Membr. Sci., 444 (2013) 327–331.
[32] J.C. Phillips, R. Braun, W. Wang, J. Gumbart, E. Tajkhorshid, E. Villa, C. Chipot, R.D. Skeel, L. Kalé, K. Schulten, Scalable molecular dynamics with NAMD, J. Comput. Chem., 26 (2005) 1781–1802.
[33] A.D. MacKerell Jr., D. Bashford, M. Bellott, R.L. Dunbrack Jr., J.D. Evanseck, M.J. Field, S. Fischer, J. Gao, H. Guo, S. Ha, All-atom empirical potential for molecular modeling and dynamics studies of proteins, J. Phys. Chem. B, 102 (1998) 3586–3616.
[34] Y. Dengfeng, L. Qingzhi, L.I. Hongman, G. Congjie, Molecular dynamics simulation of tip functionalized carbon nanotube membrane for Li^+/Mg^{2+} separation, Chin. J. Appl. Chem., 31 (2014) 1345–1351.
[35] F. Zhu, E. Tajkhorshid, K. Schulten, Pressure-induced water transport in membrane channels studied by molecular dynamics, Biophys. J., 83 (2002) 154–160.
[36] F. Zhu, E. Tajkhorshid, K. Schulten, Theory and simulation of water permeation in aquaporin-1, Biophys. J., 86 (2004) 50–57.
[37] E. Darve, D. Rodríguez-Gómez, A. Pohorille, Adaptive biasing force method for scalar and vector free energy calculations, J. Chem. Phys., 128 (2008) 144120.
[38] J. Hénin, G. Fiorin, C. Chipot, M.L. Klein, Exploring multidimensional free energy landscapes using time-dependent biases on collective variables, J. Chem. Theory Comput., 6 (2010) 35.